Supplementary Materials

Table S1. Materials used in This Study

Materials	Main components	Manufacturer
Finish	resin, aids, zinc powder, water, etc.	Hunan Xiangjiang Paint Group Co., Ltd
Diluent	ethyl acetate, butyl acetate, benzene, toluene, acetone, ethanol, butanol, etc.	
Curing agent	epoxy resin, etc.	

Table S2. Functional Groups of the Paint Mist on the Surface of Filter Elements

Wave numbers (cm^{-1})	Functional groups
2960	$-CH_3$ (methyl)
2927、1466	$-CH_2-$ (methylene)
1380	$-CH_3$（dimethyl）
1279	=C-O-C (ethers)
2853	$-O-CH_3$ (aliphatic group)
1074、1126	-C-O-C- (aliphatic group and ring)
838、743、704	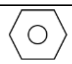 (benzene ring)
1540	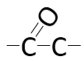 (ketone)
1729	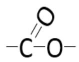 (ester)
1647	-C=C- (olefin)
3469	-OH (alcohol)

Table S3. Dimensions and Operating Parameters of Single Channel of the Baffle Interceptor

Straight section S (mm)	Bending section L (mm)	Plate spacing d (mm)	Folding angle θ (°)	Airflow velocity ν (m/s)	Particle size of paint mist D (μm)
50	100	10, 15, 20, 25, 30	60, 75, 90, 105, 120	6, 7, 8, 9, 10	1~30
Note: Plate spacing between straight sections of baffles $d^* = d / \sin\frac{\theta}{2}$					

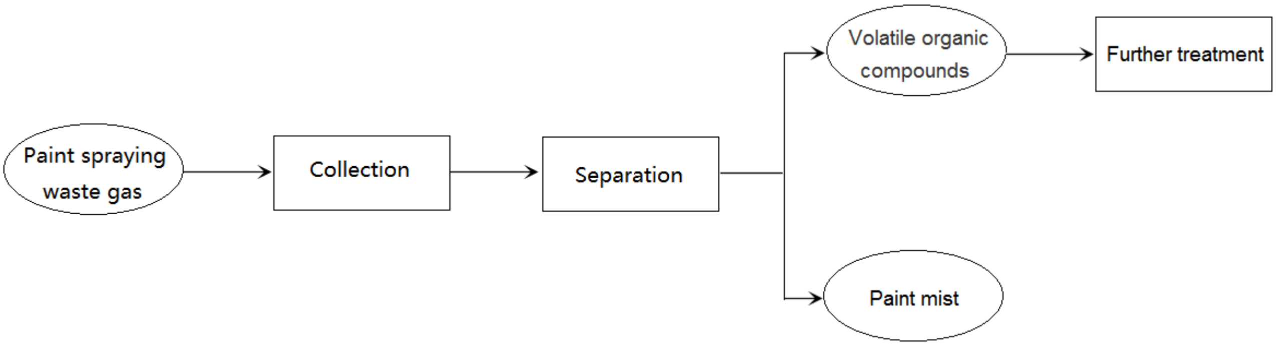

Fig. S1. The schematic illustration of the process for treating paint spraying waste gas.

Characteristic analysis, Governing equations and Mesh generation

1. Characteristic Analysis of Paint Mist

Fig. S2 presents the SEM analysis of the paint mist on the surface of filter element and the paint mist separated from the filter element. It can be seen from Fig. S2(a) that the spheres with different sizes and smaller sizes keep relatively intact shape, while the spheres with larger sizes show signs of collapse, indicating that there is a hollow structure inside the sphere, which causes collapse when subjected to force. It can be seen Fig. S2(b) that the samples are dry and there is no obvious smooth surface, shrivelled particles like raisins were observed.

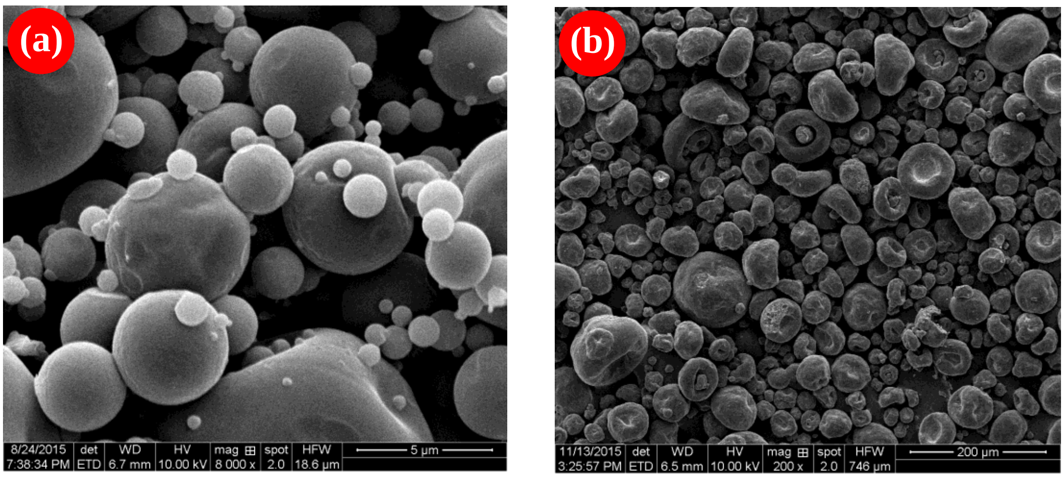

Fig. S2. SEM analysis of (a) the paint mist on the surface of filter element and (b) the paint mist separated from the filter element.

2. Governing Equations

2.1. Gas phase Turbulence Control Equation

The continuous equation, momentum equations, Navier-Stokes equation, *k*-*ε* equation of continuous phase is described as：

$$\frac{\partial(\rho u)}{\partial x}+\frac{\partial(\rho v)}{\partial y}=0 \tag{1}$$

$$\frac{\partial(\rho uu)}{\partial x}+\frac{\partial(\rho vu)}{\partial y}=-\frac{\partial P}{\partial x}+\frac{\partial}{\partial x}\left(2\mu\frac{\partial u}{\partial x}\right)+\frac{\partial}{\partial y}\left[\mu\left(\frac{\partial u}{\partial y}+\frac{\partial v}{\partial x}\right)\right] \tag{2}$$

$$\frac{\partial(\rho uv)}{\partial x}+\frac{\partial(\rho vv)}{\partial y}=-\frac{\partial P}{\partial y}+\frac{\partial}{\partial x}\left[\mu\left(\frac{\partial u}{\partial y}+\frac{\partial v}{\partial x}\right)\right]+\frac{\partial}{\partial y}\left[2\mu\frac{\partial v}{\partial y}\right] \tag{3}$$

Where ρ is the density of gas; u and v are velocity components in x and y directions, μ is the viscosity of the gas phase, p is the pressure on the fluid micro-element.

$$\frac{\partial}{\partial x_i}(\rho k u_i)=\frac{\partial}{\partial x_j}\left[\left(\mu+\frac{\mu_t}{\sigma_k}\right)\frac{\partial k}{\partial x_j}\right]+G_k+G_b-\rho\varepsilon-Y_M+S_k \tag{4}$$

$$\frac{\partial}{\partial x_i}(\rho\varepsilon u_i)=\frac{\partial}{\partial x_j}\left[\left(\mu+\frac{\mu_t}{\sigma_\varepsilon}\right)\frac{\partial\varepsilon}{\partial x_j}\right]+C_{1\varepsilon}\frac{G}{k}(G_k+C_{3\varepsilon}G_b)-C_{2\varepsilon}\rho\frac{\varepsilon^2}{k}+S_\varepsilon \tag{5}$$

In the equation, G_k represents the turbulent flow energy generated by the laminar velocity gradient, G_b is the turbulent flow energy generated by buoyancy; Y_M is the fluctuation due to the transition of the transition in the compressible turbulent flow. C_1, C_2 and C_3 are constants, σ_k and σ_ε are the turbulent Prandtl numbers for k and ε respectively, S_k and S_ε are user-defined source terms. These constants are set as follows: $\sigma_k = 1.0$, $\sigma_\varepsilon = 1.3$, $C_{1\varepsilon} = 1.44$, $C_{2\varepsilon} = 1.92$, and $C_{3\varepsilon} = 0.09$.

2.2. Discrete Phase Track Computation Equation

Discrete phase particle trajectories were predicted by using the Discrete Phase Model (DPM) model based on the Euler-Lagrange approach. The force balance equates the particle inertia with the force acting on the particle, and can be written as:

$$\frac{du_p}{dt}=\frac{18\mu}{\rho_p D_p^{\,2}}\cdot\frac{C_D\,\mathrm{Re}}{24}(u-u_p)+F_x \tag{6}$$

Where u is the gas phase velocity, U_p is the particle's velocity, μ is the molecular of the gas phase, ρ is the gas phase density, ρ_p is the density of the particles and D_p is the particle's diameter. Re is the relative Reynolds number, Fx is the other forces in the calculation process.

3. Mesh Generation

The model of the single channel (the folding angle is 90°, the plate spacing is 20 mm) was established and the geometry was structurally meshed, as shown in Fig. S5 and Fig. S6. Since the majority of separated paint mist particles are expected to form a liquid film on the walls of the channel, finer grids were generated near the wall region, to achieve precise results. In order to obtain the accurate calculation results, the calculation domain was divided into a finite number of control volumes (about 55000 cells).

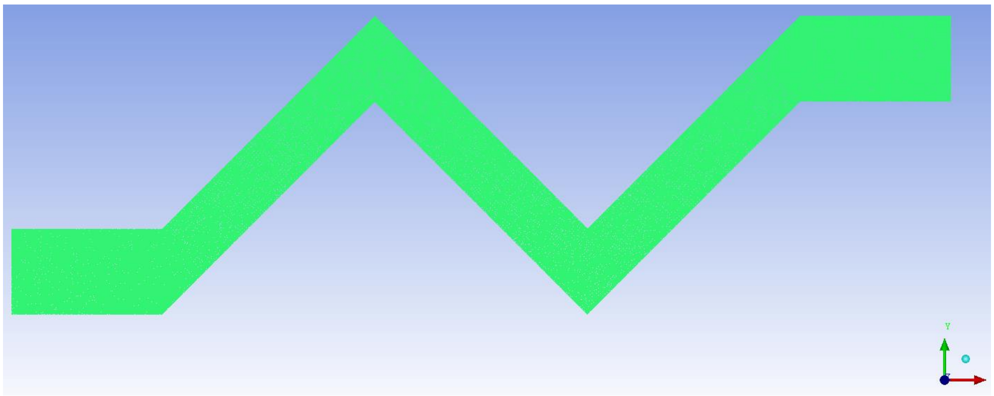

Fig. S3. The model of single channel of the baffle interceptor.

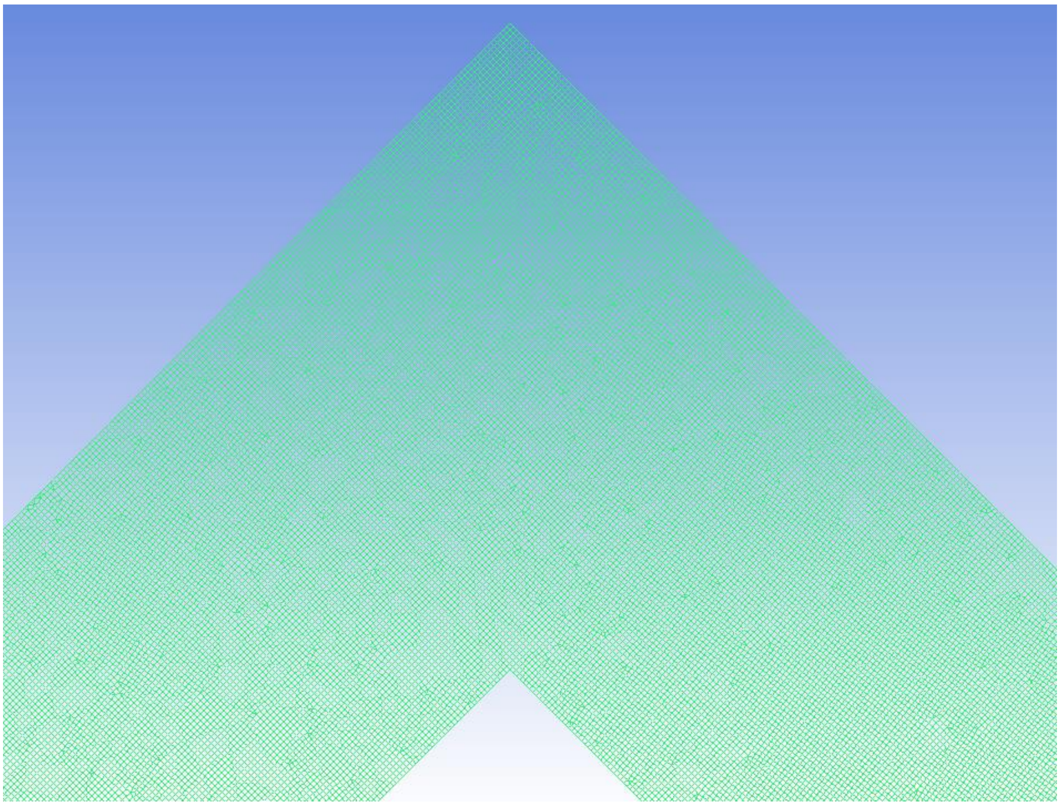

Fig. S4. The computational grids of the single channel.

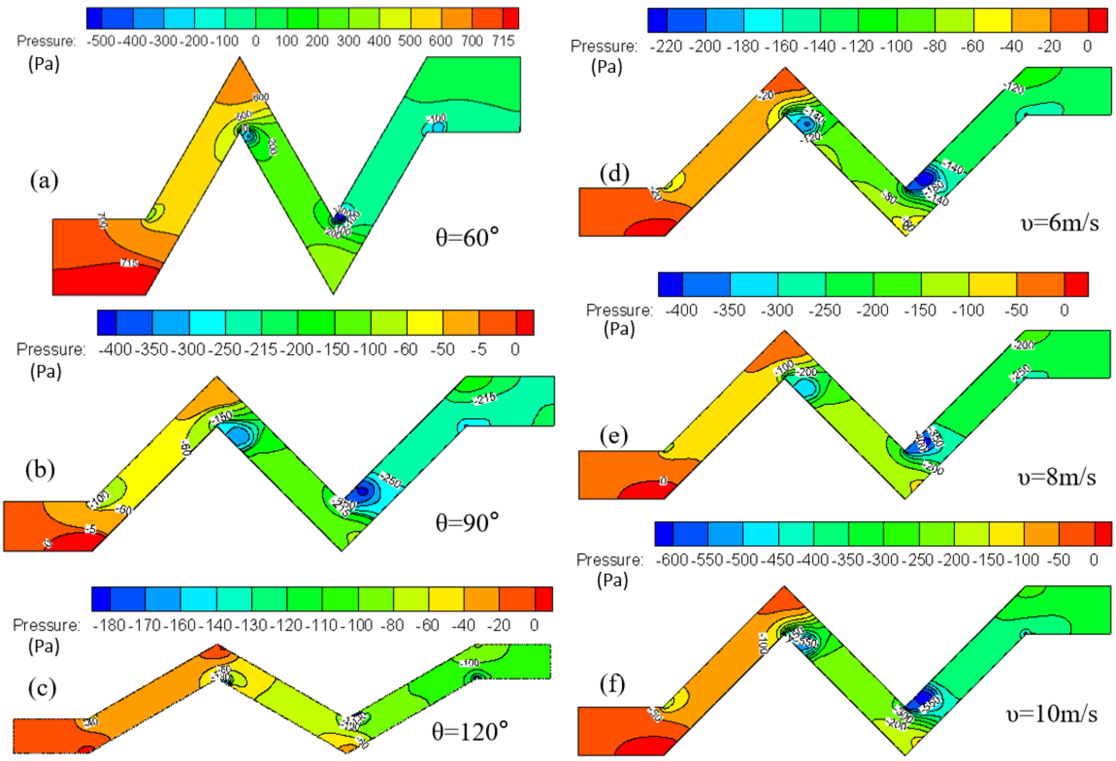

Fig. S5. The Pressure profile in the channel of the baffle interceptor: (a), (b), (c) different folding angles; (d), (e), (f) different airflow velocities.

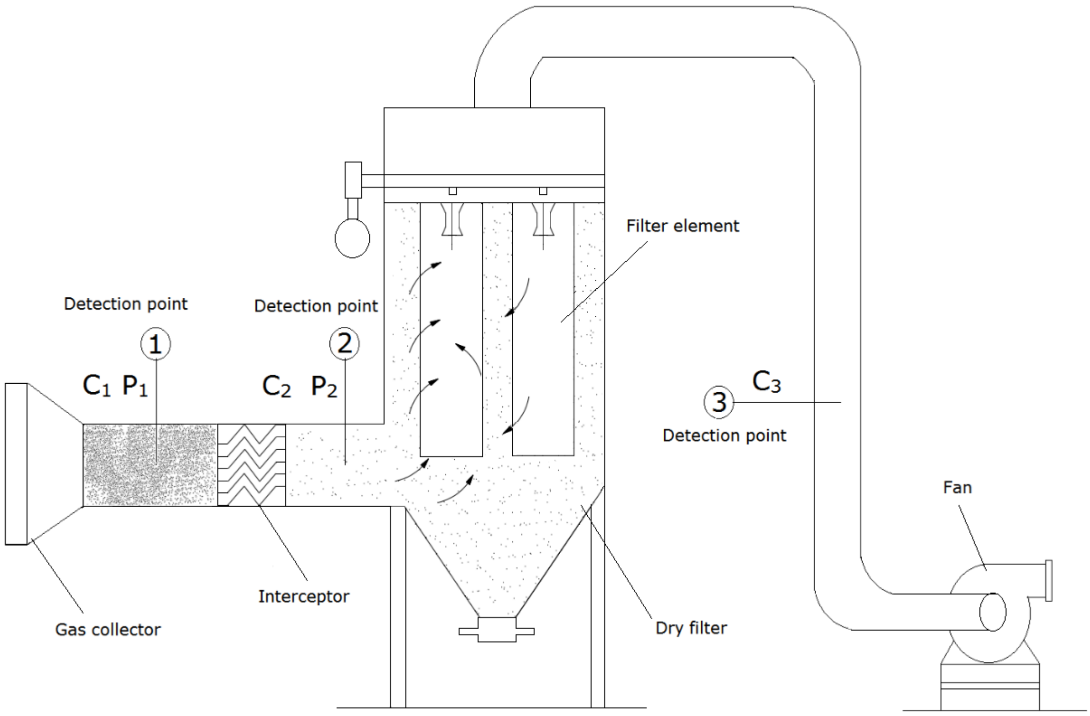

Fig. S6. The schematic illustration of interception-filtration coupling device.

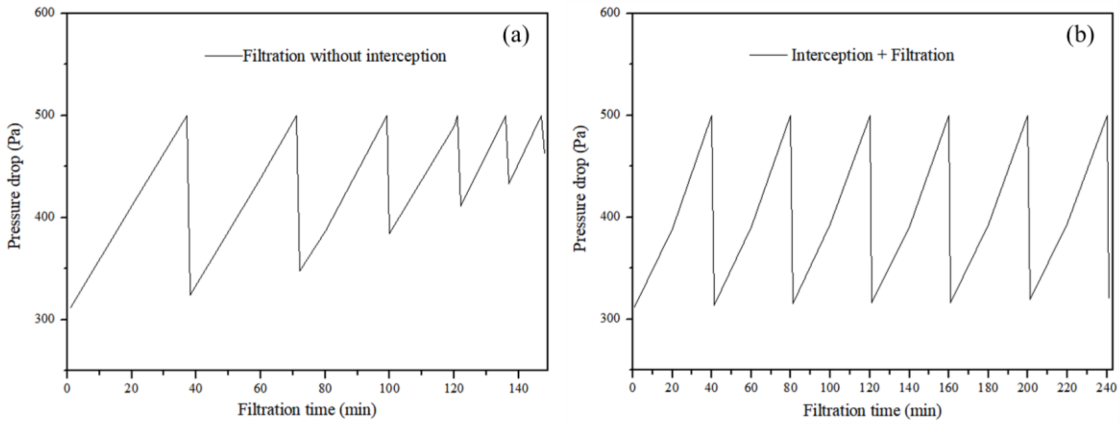

Fig. S7. Filter pressure drop over time.

The back-flushing pressure was set at 500 Pa. If the pressure loss of the filter is overpass 500 Pa, a backflushing procedure (for filter cleaning) will be performed.